Mathematics

http://www.aimspress.com/journal/Math

AIMS Mathematics, 10(10): 24997–25010.
DOI: 10.3934/math.20251107
Received: 17 September 2025
Revised: 25 October 2025
Accepted: 28 October 2025
Published: 31 October 2025

Research article

The impact of standard Wiener process on the qualitative analysis and traveling wave solutions of stochastic nonlinear Kodama equation in the Stratonovich sense

Jin Wang and Zhao Li*

College of Computer Science, Chengdu University, Chengdu, 610106, China

* **Correspondence:** Email: lizhao@cdu.edu.cn.

Abstract: This article investigates the qualitative analysis and traveling wave solutions of the stochastic nonlinear Kodama equation within the Stratonovich framework. By applying a random traveling wave transformation, the equation is first converted into an ordinary differential equation. The qualitative behavior of the corresponding two-dimensional dynamical system and its perturbation is then examined using planar dynamical system analysis. Subsequently, the complete discriminant system method is employed to derive four distinct types of optical solutions. Three-dimensional plots illustrating these solutions under different parameters are also presented.

Keywords: nonlinear Kodama equation; traveling wave solution; traveling wave transformation; stochastic; planar dynamical system
Mathematics Subject Classification: 34H20, 35B20, 35C05, 35C07

1. Introduction

As is well known, stochastic partial differential equations (SPDEs) [1–3] are commonly used for nonlinear phenomena in fields such as physics, economics, biology, communication, and engineering technology [4–6]. Currently, research on SPDEs mainly focuses on the existence and uniqueness of solutions, martingale solutions, numerical solutions, and analytical solutions. In fact, the problems of the existence, uniqueness, and martingale solutions of SPDEs have been solved. Moreover, in recent years, many experts and scholars have also proposed machine learning methods and numerical analysis methods [7–9]. However, the construction of analytical solutions for SPDEs has always been a hot topic [10, 11]. The main reasons can be attributed to the following three points: Firstly, due to the complexity of stochastic problems, there is no unified method to construct analytical solutions for SPDEs. Secondly, the Itô formula cannot be directly applied to SPDEs. Thirdly, the types of random noise are also very complex. Based on the above considerations, the main purpose of this article is to study the analytical solutions and dynamic behavior of a class of SPDEs.

The stochastic nonlinear Kodama (SNLK) equation in the Stratonovich sense is described as follows [12, 13]

$$i\mathfrak{u}_t + \mathfrak{u}_{xx} + i\mathfrak{u}_{xxx} + \gamma_1|\mathfrak{u}|^2 u + i\gamma_2|\mathfrak{u}|^2\mathfrak{u}_x + i\gamma_3\mathfrak{u}^2\mathfrak{u}_x^* = i\sigma\mathfrak{u} \circ w_t, \tag{1.1}$$

where $\mathfrak{u} = \mathfrak{u}(x,t)$ is the complex function. t and x represent time and spatial variables, respectively. Parameters γ_1, γ_2, and γ_3 are arbitrary constants. σ represents the noise amplitude. $w = w(t)$ stands for the standard Wiener process, and $w_t = \frac{dw}{dt}$. The standard Brownian motion can be referred to in reference [14]. i represents the imaginary unit satisfying $i^2 = -1$. $\mathfrak{u}^*$ represents the conjugate complex function of $\mathfrak{u}$. $|\cdot|$ represents the modulus of the complex number $\mathfrak{u}$. In reference [12], Algolam and his collaborators studied the traveling wave solutions of Eq (1.1) by using (G'/G)-expansion method and mapping method, respectively. In reference [13], Sağlam used Kumar-Malik and Polynomial expansion methods to study the traveling wave solutions of Eq (1.1), and obtained three-dimensional and two-dimensional partial solutions through numerical simulations. However, the study of Eq (1.1) remains a very hot topic in current research. This article will focus on the study of traveling wave solutions and qualitative theory for Eq (1.1). The main highlights of this article are three points: The first point is that this article uses the complete discriminant system method to construct the soliton solution of Eq (1.1). Secondly, this article presents the model of Eq (1.1) and its perturbation of the two-dimensional dynamical system [15]. Thirdly, this article investigates the planar phase diagram, bifurcation diagram, and maximum Lyapunov exponent diagram of Eq (1.1) and its perturbed system.

The subsequent sections are arranged as follows: In Section 2, the SNLK equation is transformed into a nonlinear ordinary differential equation. In Section 3, the qualitative behavior of two-dimensional dynamical systems and their perturbation systems is studied. In Section 4, four types of optical solutions of the SNLK equation are constructed. In Section 5, the three-dimensional diagrams of its optical solutions of the SNLK equation are also drawn. In Section 6, a brief conclusion is given.

2. Preliminary

Lemma 2.1. *[12]* $\mathbb{E}(e^{\sigma w(t)}) = e^{\frac{1}{2}\sigma^2 t}$ *for any positive real number* σ.

The Stratonovich integral and Itô integral satisfy the following relationship (see Ref. [12])

$$\int_0^t G(s,Z_s) \circ dw(s) = \int_0^t G(s,Z_s)dw(s) + \frac{1}{2}\int_0^t G(s,Z_s)\frac{\partial G(s,Z_s)}{\partial s}ds, \tag{2.1}$$

where $\{Z_s, t \leq 0\}$ is a stochastic process and G is assumed to be sufficiently regular.

Next, let's perform a traveling wave transformation

$$\mathfrak{u}(x,t) = \mathcal{U}(\zeta)e^{i(\chi_1 x+\chi_2 t)+\sigma w(t)-\sigma^2 t},\ \zeta = \zeta_1 x + \zeta_2 t, \tag{2.2}$$

where $\mathcal{U}(\zeta)$ represents the deterministic real function. ζ_1, ζ_2, χ_1 and χ_2 are nonzero constants. This section considers a traveling wave transformation with randomness, which was first proposed by Mohammed et al. [16], and its wave transformation has been widely used in solving traveling wave solutions of SPDEs this year. Much literature has already reported on this type of transformation.

By calculating the various derivatives of u, we can obtain

$$
\begin{aligned}
&u_t = (\zeta_2\mathcal{U}' + i\chi_2\mathcal{U} + \sigma\mathcal{U}\circ w_t)e^{i(\chi_1 x+\chi_2 t)+\sigma w(t)-\sigma^2 t},\\
&u_x = (\zeta_1\mathcal{U}' + i\chi_1\mathcal{U})e^{i(\chi_1 x+\chi_2 t)+\sigma w(t)-\sigma^2 t},\\
&u_{xx} = (\zeta_1^2\mathcal{U}'' + 2i\chi_1\zeta_1\mathcal{U}' - \chi_1^2\mathcal{U})e^{i(\chi_1 x+\chi_2 t)+\sigma w(t)-\sigma^2 t},\\
&u_{xxx} = (\zeta_1^3\mathcal{U}''' + 3i\chi_1\zeta_1^2\mathcal{U}'' - 3\chi_1^2\zeta_1\mathcal{U}' - i\chi_1^3\mathcal{U})e^{i(\chi_1 x+\chi_2 t)+\sigma w(t)-\sigma^2 t}.
\end{aligned}
\tag{2.3}
$$

Substituting Eq (2.3) into Eq (1.1) and separating the real and imaginary parts, taking the expectation $\mathbb{E}(\cdot)$ and combining them with Lemma 2.1, we can obtain a deterministic ordinary differential equation

$$
\begin{aligned}
&\text{Imaginary part}: \gamma_1\zeta_1^3\mathcal{U}''' + (\zeta_2 + 2\chi_1\zeta_1 - 3\gamma_1\chi_1^2\zeta_1)\mathcal{U}' + \zeta_1(\gamma_2+\gamma_3)\mathcal{U}^2\mathcal{U}' = 0,\\
&\text{Real part}: (\zeta_1^2 - 3\gamma_1\chi_1\zeta_1^2)\mathcal{U}'' + (\gamma_1\chi_1^3 - \chi_2 - \chi_1^2)\mathcal{U} + (\gamma_1 - \gamma_2\chi_1 + \gamma_3\chi_1)\mathcal{U}^3 = 0.
\end{aligned}
\tag{2.4}
$$

Integrating both sides of Eq (2.4) with respect to ξ simultaneously once and setting the integration constant to zero yields

$$
\gamma_1\zeta_1^3\mathcal{U}'' + (\zeta_2 + 2\chi_1\zeta_1 - 3\gamma_1\chi_1^2\zeta_1)\mathcal{U} + \frac{\zeta_1(\gamma_2+\gamma_3)}{3}\mathcal{U}^3 = 0. \tag{2.5}
$$

The second equation of Eq (2.4) is equivalent to Eq (2.5) and must satisfy the following conditions:

$$
\frac{1-3\gamma_1\chi_1}{\gamma_1\zeta_1} = \frac{\gamma_1\chi_1^3 - \chi_2 - \chi_1^2}{\zeta_2 + 2\chi_1\zeta_1 - 3\gamma_1\chi_1^2\zeta_1} = \frac{3(\gamma_1 - \gamma_2\chi_1 + \gamma_3\chi_1)}{\zeta_1(\gamma_2+\gamma_3)}. \tag{2.6}
$$

If the conditions of Eq (2.6) are satisfied, then, Eq (2.5) can be rewritten as

$$
\mathcal{U}'' + \vartheta_2\mathcal{U}^3 + \vartheta_1\mathcal{U} = 0, \tag{2.7}
$$

where $\vartheta_2 = \frac{\gamma_2+\gamma_3}{3\gamma_1\zeta_1^2}$ and $\vartheta_1 = \frac{\zeta_2+2\chi_1\zeta_1-3\gamma_1\chi_1^2\zeta_1}{\gamma_1\zeta_1^3}$.

3. Qualitative analysis

In reference [17], Hosseini et al. have studied the dynamic behavior of the nonlinear Kodama equation by using the planar dynamical system method. In this article, we first assume that $\frac{d\mathcal{U}}{d\xi} = z$, two-dimensional dynamical system of Eq.(2.7) can be described as follows

$$
\begin{cases}
\frac{d\mathcal{U}}{d\zeta} = z,\\
\frac{dz}{d\zeta} = -\vartheta_2\mathcal{U}^3 - \vartheta_1\mathcal{U}.
\end{cases}
\tag{3.1}
$$

In the section, we consider Eq (1.1) as a small perturbation system as follows

$$
iu_t + u_{xx} + iu_{xxx} + \gamma_1|u|^2u + i\gamma_2|u|^2u_x + i\gamma_3u^2u_x^* = i\sigma u\circ w_t + F(u), \tag{3.2}
$$

where F is a function with small perturbation.

By applying all the traveling wave transformations in Section 2 to Eq (3.2), we assume that $F = (\zeta_1^2 - 3\gamma_1\chi_1\zeta_1^2)f$. We obtain a perturbation to Eq (3.1) that is different from the small perturbation in reference [17].

$$\begin{cases} \frac{d\mathcal{U}}{d\zeta} = z, \\ \frac{dz}{d\zeta} = -\vartheta_2\mathcal{U}^3 - \vartheta_1\mathcal{U} + f(\zeta), \end{cases} \tag{3.3}$$

where $f(\zeta) = f_0\sin(k\zeta) + h_0\cos(l\zeta)$ or $f(\zeta) = g_0e^{k\zeta}$.

In this section, we plot the two-dimensional and three-dimensional phase diagrams of system (3.3) with different initial values. In Figures 1–4, Figures 1(c)–4(c), the disturbance system is a small periodic disturbance system, where the red and blue orbits represent different initial values; the initial value of the red orbit is $\mathcal{U}(0) = 1$, $z = 0$; the initial value of the blue orbit is $\mathcal{U}(0) = 0$, $z = 0$. From the figures, we can conclude that system (3.3) will exhibit chaotic behavior under small periodic disturbance systems. The disturbance system considered in Figures 1(b)–4 (b) is a small exponential disturbance, and the dynamic behavior of the system varies for different initial values. As shown in Figure 5, when the Poincaré section is a closed curve, it can be determined that the system (3.3) is quasi periodic. As shown in Figure 6, when there are dense points on the Poincaré section and a hierarchical structure, it can be determined that system (3.3) is in a chaotic state. In Figures 7–9, we plot the bifurcation and Lyapunov exponent of Eq (3.3), respectively. As shown in Figure 7, bifurcation behavior refers to the phenomenon where the qualitative structure of a dynamical system undergoes sudden changes with parameter variations. In this article, Figure 7 shows the bifurcation diagram of the system as the parameter r (defined as $r = \sqrt{z^2 + \mathcal{U}^2}$) varies. The dense regions and discontinuous changes at the points in the bifurcation diagram indicate the existence of a transition between chaotic and periodic states in the system. For example, when r passes a specific critical value, the system may transition from periodic oscillation to chaotic behavior. As shown in Figures 8 and 9, if the maximum Lyapunov exponent is positive, it indicates that the adjacent orbital exponents are separated and the system is in a chaotic state. The positive exponents of some intervals in Figures 8 and 9 confirm the existence of chaos in the perturbed system (3.3). As shown in Figures 10 and 11, the sensitivity analysis of system (3.3) is presented. Sensitivity analysis refers to the study of how significant differences in the long-term behavior of a system (3.3) can occur when there are extremely small changes in initial conditions or system parameters. When the initial conditions are fixed, observe how the long-term behavior of the system (such as amplitude and periodicity/chaos) changes when a parameter of the system undergoes a small change. If the maximum Lyapunov exponent is positive, it proves that the system is chaotic and sensitive to initial conditions. The magnitude of this index directly reflects the average rate of trajectory separation.

Remark 3.1. *Compared with reference [17], the disturbances of the perturbation system (3.3) considered in this paper are two different functions, one is $f(\zeta) = f_0\sin(k\zeta) + h_0\cos(l\zeta)$, and the other is $f(\zeta) = g_0e^{k\zeta}$. However, reference [17] only discusses the perturbation system as $f(\zeta) = h_0\cos(l\zeta)$. This paper also adds the bifurcation and maximum Lyapunov exponent of system (3.3).*

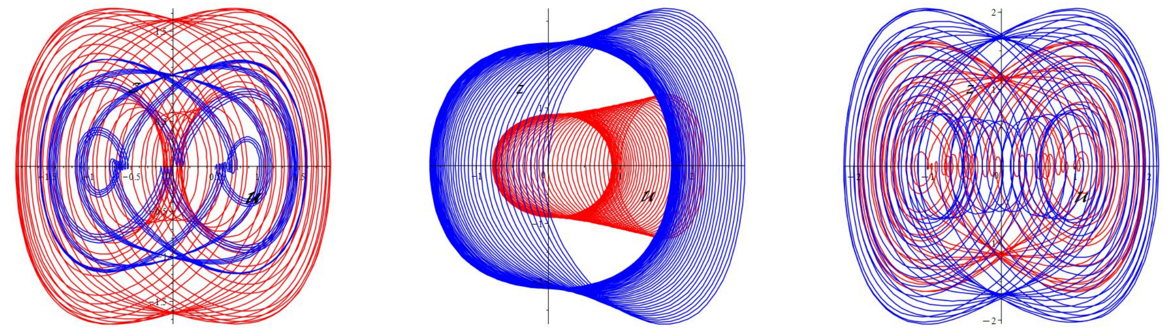

(a) $f = 1.2\sin(0.6\zeta)$ (b) $f = 3.6e^{-0.02\zeta}$ (c) $f = 1.2\sin(0.6\zeta) + 1.2\cos(0.6\zeta)$

Figure 1. Two-dimensional phase portraits of Eq (3.3) for $\vartheta_1 = 1, \vartheta_2 = \frac{3}{7}, \gamma_1 = 1, \gamma_2 = 1, \gamma_3 = \frac{2}{7}, \chi_1 = -1, \chi_2 = -2, \zeta_1 = 1, \zeta_2 = 6$.

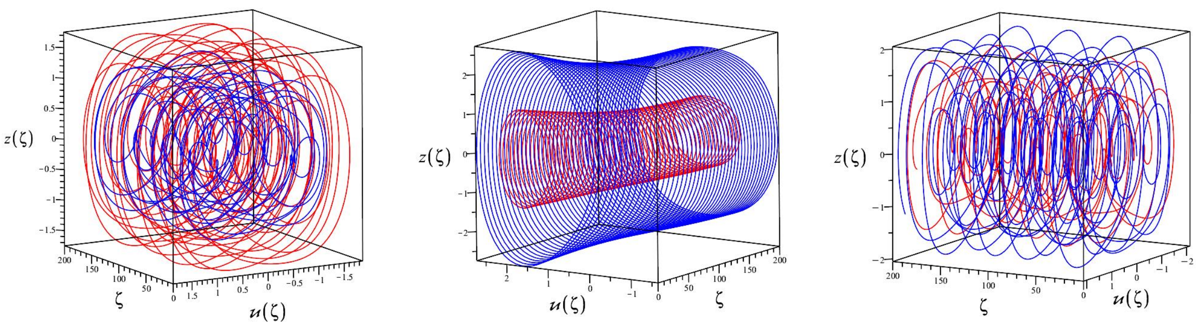

(a) $f = 1.2\sin(0.6\zeta)$ (b) $f = 3.6e^{-0.02\zeta}$ (c) $f = 1.2\sin(0.6\zeta) + 1.2\cos(0.6\zeta)$

Figure 2. Three-dimensional phase portraits of Eq (3.3) for $\vartheta_1 = 1, \vartheta_2 = \frac{3}{7}, \gamma_1 = 1, \gamma_2 = 1, \gamma_3 = \frac{2}{7}, \chi_1 = -1, \chi_2 = -2, \zeta_1 = 1, \zeta_2 = 6$.

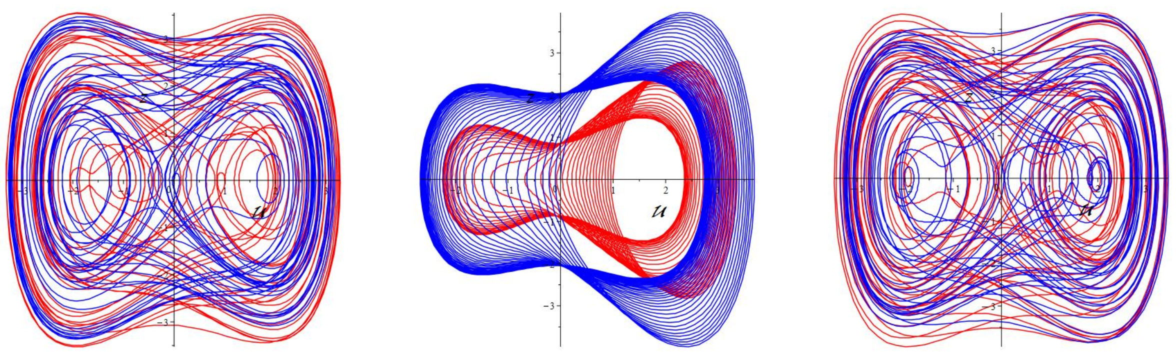

(a) $f = 1.2\sin(0.6\zeta)$ (b) $f = 3.6e^{-0.02\zeta}$ (c) $f = 1.2\sin(0.6\zeta) + 1.2\cos(0.6\zeta)$

Figure 3. Two-dimensional phase portraits of Eq (3.3) for $\vartheta_1 = 1, \vartheta_2 = \frac{3}{7}, \gamma_1 = 1, \gamma_2 = 1, \gamma_3 = \frac{2}{7}, \chi_1 = -1, \chi_2 = 1, \zeta_1 = -1, \zeta_2 = -4$.

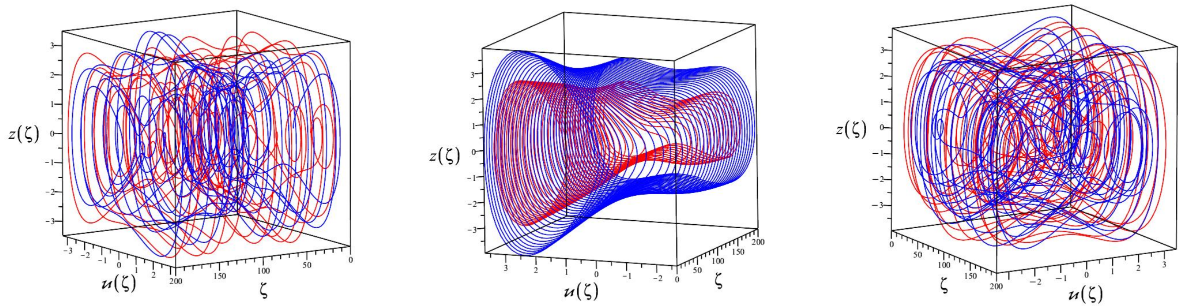

(a) $f = 1.2\sin(0.6\zeta)$ (b) $f = 3.6e^{-0.02\zeta}$ (c) $f = 1.2\sin(0.6\zeta) + 1.2\cos(0.6\zeta)$

Figure 4. Three-dimensional phase portraits of Eq (3.3) for $\vartheta_1 = 1, \vartheta_2 = \frac{3}{7}, \gamma_1 = 1, \gamma_2 = 1, \gamma_3 = \frac{2}{7}, \chi_1 = -1, \chi_2 = 1, \zeta_1 = -1, \zeta_2 = -4$.

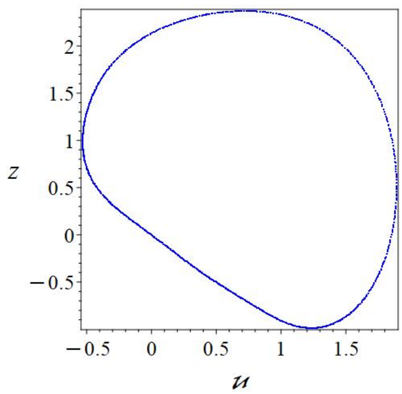

Figure 5. Poincaré section of Eq (3.3) for $\vartheta_1 = 1, \vartheta_2 = \frac{3}{7}, \gamma_1 = 1, \gamma_2 = 1, \gamma_3 = \frac{2}{7}, \chi_1 = -1, \chi_2 = -2, \zeta_1 = 1, \zeta_2 = 6$, $f = 1.2\sin(0.6\zeta) + 1.2\cos(0.6\zeta)$.

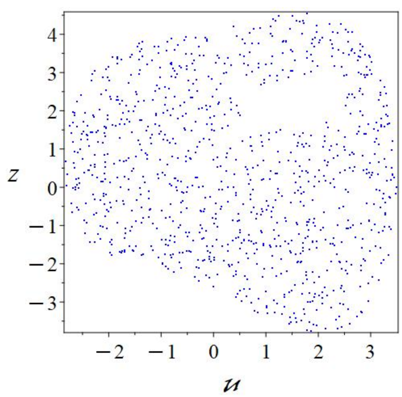

Figure 6. Poincaré section of Eq (3.3) for $\vartheta_1 = 1, \vartheta_2 = \frac{3}{7}, \gamma_1 = 1, \gamma_2 = 1, \gamma_3 = \frac{2}{7}, \chi_1 = -1, \chi_2 = 1, \zeta_1 = -1, \zeta_2 = -4$, $f = 1.2\sin(0.6\zeta) + 1.2\cos(0.6\zeta)$.

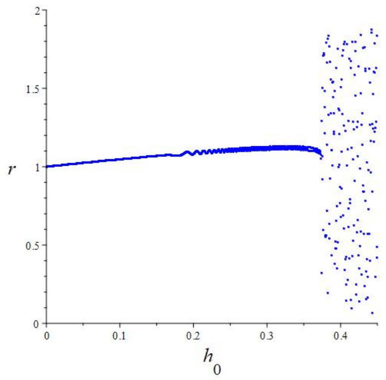

(a) $h_0 = 0.2$

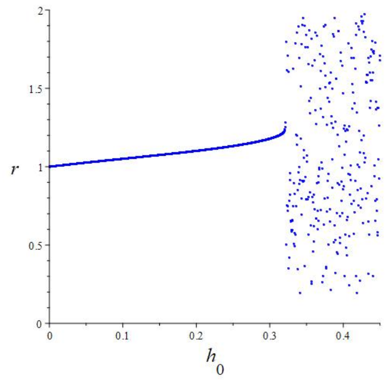

(b) $h_0 = 0.4$

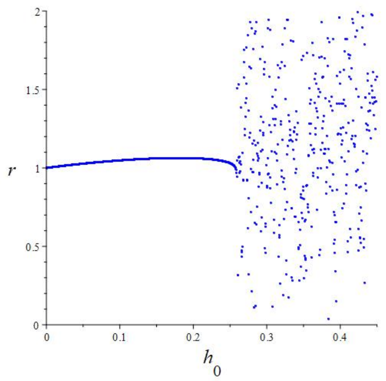

(c) $h_0 = 0.6$

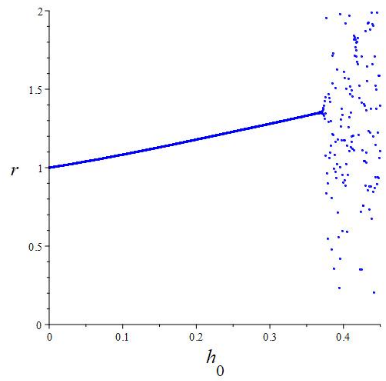

(d) $h_0 = 0.8$

Figure 7. The bifurcation of Eq (3.3) for $\vartheta_2 = 1, \vartheta_1 = -1, r = \sqrt{z^2 + \mathcal{U}^2}$.

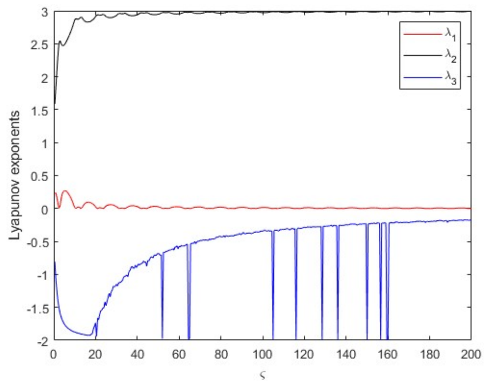

Figure 8. Lyapunov exponents of Eq (3.3) for $\vartheta_1 = 1, \vartheta_2 = \frac{3}{7}, \gamma_1 = 1, \gamma_2 = 1, \gamma_3 = \frac{2}{7}, \chi_1 = -1, \chi_2 = -2, \zeta_1 = 1, \zeta_2 = 6, f = 1.2\sin(\zeta) + 1.2\cos(\zeta)$.

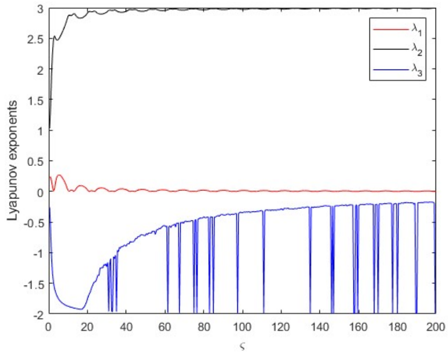

Figure 9. Lyapunov exponents of Eq (3.3) for $\vartheta_1 = 1, \vartheta_2 = \frac{3}{7}, \gamma_1 = 1, \gamma_2 = 1, \gamma_3 = \frac{2}{7}, \chi_1 = -1, \chi_2 = 1, \zeta_1 = -1, \zeta_2 = -4$, $f = 1.2\sin(\zeta) + 1.2\cos(\zeta)$.

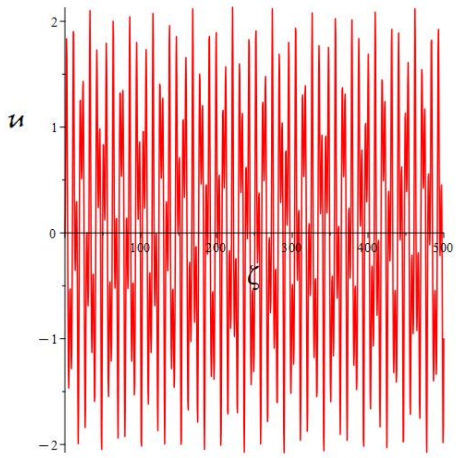

Figure 10. Sensitivity analysis of Eq (3.3) for $\vartheta_1 = 1, \vartheta_2 = \frac{3}{7}, \gamma_1 = 1, \gamma_2 = 1, \gamma_3 = \frac{2}{7}, \chi_1 = -1, \chi_2 = -2, \zeta_1 = 1, \zeta_2 = 6$, $f = 1.2\sin(0.6\zeta) + 1.2\cos(0.6\zeta)$.

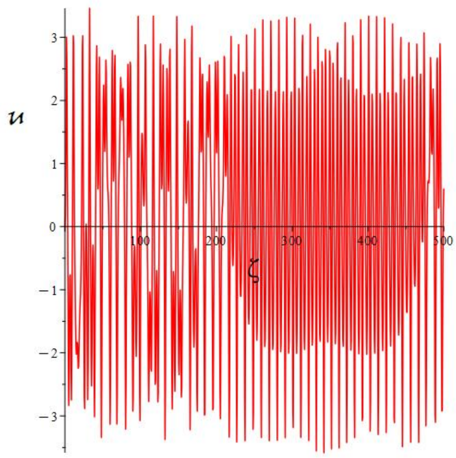

Figure 11. Sensitivity analysis of Eq (3.3) for $\vartheta_1 = 1, \vartheta_2 = \frac{3}{7}, \gamma_1 = 1, \gamma_2 = 1, \gamma_3 = \frac{2}{7}, \chi_1 = -1, \chi_2 = 1, \zeta_1 = -1, \zeta_2 = -4$, $f = 1.2\sin(0.6\zeta) + 1.2\cos(0.6\zeta)$.

4. Traveling wave solutions of SNLK equation

Multiply both sides of Eq (2.7) by $\mathcal{U}'$ integral once, and simplify it to obtain

$$(\mathcal{U}')^2 = -\frac{\vartheta_2}{2}\mathcal{U}^4 - \vartheta_1\mathcal{U}^2 + 2\vartheta_0, \tag{4.1}$$

where ϑ_0 is an integral constant.

In order to obtain the optical solutions, we make the following assumptions:

$$\mathcal{U} = \pm\sqrt{(-2\vartheta_2)^{-\frac{1}{3}}\Xi},\ \ \eta_1 = -4\vartheta_1(-2\vartheta_2)^{-\frac{2}{3}},\ \ \eta_0 = 8\vartheta_0(-2\vartheta_2)^{-\frac{1}{3}},\ \ \xi_1 = (-2\vartheta_2)^{\frac{1}{3}}\zeta. \tag{4.2}$$

Then, Eq (4.1) can be rewritten as

$$(\Xi_{\xi_1})^2 = \Xi(\Xi^2 + \eta_1\Xi + \eta_0). \tag{4.3}$$

Here, we assume that $F(\Xi) = \Xi^2 + \eta_1\Xi + \eta_0$, its discriminant can be expressed as $\Delta = \eta_1^2 - 4\eta_0$. Thus, the integral expression of Eq (4.3) can be expressed as

$$\pm(\xi_1 - \xi_0) = \int \frac{d\Xi}{\sqrt{\Xi(\Xi^2 + \eta_1\Xi + \eta_0)}}. \tag{4.4}$$

Indeed, much literature is using the fully discriminative system method to construct traveling wave solutions for nonlinear partial differential equations and fractional-order partial differential equations. However, there is still limited literature on the construction of traveling wave solutions for stochastic nonlinear partial differential equations based on the complete discriminative system method. This method, which was first proposed by Professor Liu can be referred to in reference [18]. The complete discriminant system method for polynomials considers that the right-hand end of Eq (4.1) is a polynomial, and the solutions of complete discriminant systems for second-order, third-order, fourth-order, and fifth-order polynomials can be obtained. Even for some special high-order equations, their solutions can be obtained by simplification. According to the complete discriminant system method of polynomials [18], we can easily obtain all solutions of Eq (4.4), so that we can obtain the solution of Eq (1.1) in the following four situations:

Case 1. $\Delta = \eta_1^2 - 4\eta_0 = 0$, $\Xi > 0$.

If $\eta_1 < 0$, we can obtain the solution of Eq (1.1) by integrating Eq (4.4)

$$\mathrm{u}_1(x,t) = \pm\sqrt{-\frac{\vartheta_1}{\vartheta_2}}|\tanh(\frac{\sqrt{2\vartheta_1(-2\vartheta_2)^{-\frac{2}{3}}}}{2}((-2\vartheta_2)^{\frac{1}{3}}(\zeta_1 x + \zeta_2 t) - \xi_0))|e^{i(\chi_1 x+\chi_2 t)+\sigma w(t)-\sigma^2 t}. \tag{4.5}$$

$$\mathrm{u}_2(x,t) = \pm\sqrt{-\frac{\vartheta_1}{\vartheta_2}}|\coth(\frac{\sqrt{2\vartheta_1(-2\vartheta_2)^{-\frac{2}{3}}}}{2}((-2\vartheta_2)^{\frac{1}{3}}(\zeta_1 x + \zeta_2 t) - \xi_0))|e^{i(\chi_1 x+\chi_2 t)+\sigma w(t)-\sigma^2 t}. \tag{4.6}$$

If $\eta_1 > 0$, we can obtain the solution of Eq (1.1) by integrating Eq (4.4)

$$\mathrm{u}_3(x,t) = \pm\sqrt{\frac{\vartheta_1}{\vartheta_2}}|\tan(\frac{\sqrt{-2\vartheta_1(-2\vartheta_2)^{-\frac{2}{3}}}}{2}((-2\vartheta_2)^{\frac{1}{3}}(\zeta_1 x + \zeta_2 t) - \xi_0))|e^{i(\chi_1 x+\chi_2 t)+\sigma w(t)-\sigma^2 t}. \tag{4.7}$$

If $\eta_1 = 0$, we can obtain the solution of Eq (1.1) by integrating Eq (4.4)

$$\mathrm{u}_4(x,t) = \pm\sqrt{(-2\vartheta_2)^{-\frac{1}{3}}}\left|\frac{2}{|(-2\vartheta_2)^{\frac{1}{3}}(\zeta_1 x+\zeta_2 t)-\xi_0|}\right|e^{i(\chi_1 x+\chi_2 t)+\sigma w(t)-\sigma^2 t}. \tag{4.8}$$

Case 2. $\Delta = \eta_1^2 - 4\eta_0 > 0$, $\eta_0 = 0$, $\Xi > -\zeta_1$.

If $\eta_1 > 0$, we can obtain the solution of Eq (1.1) by integrating Eq (4.4)

$$\mathrm{u}_5(x,t) = \pm\sqrt{\frac{\vartheta_1}{\vartheta_2}\tanh^2(\frac{\sqrt{-2\vartheta_1(-2\vartheta_2)^{-\frac{2}{3}}}}{2}((-2\vartheta_2)^{\frac{1}{3}}(\zeta_1 x+\zeta_2 t)-\xi_0))-\frac{2\vartheta_1}{\vartheta_2}}e^{i(\chi_1 x+\chi_2 t)+\sigma w(t)-\sigma^2 t}. \tag{4.9}$$

$$\mathrm{u}_6(x,t) = \pm\sqrt{\frac{\vartheta_1}{\vartheta_2}\coth^2(\frac{\sqrt{-2\vartheta_1(-2\vartheta_2)^{-\frac{2}{3}}}}{2}((-2\vartheta_2)^{\frac{1}{3}}(\zeta_1 x+\zeta_2 t)-\xi_0))-\frac{2\vartheta_1}{\vartheta_2}}e^{i(\chi_1 x+\chi_2 t)+\sigma w(t)-\sigma^2 t}. \tag{4.10}$$

If $\eta_1 < 0$, we can obtain the solution of Eq (1.1) by integrating Eq (4.4)

$$\mathrm{u}_7(x,t) = \pm\sqrt{-\frac{\vartheta_1}{\vartheta_2}\tan^2(\frac{\sqrt{2\vartheta_1(-2\vartheta_2)^{-\frac{2}{3}}}}{2}((-2\vartheta_2)^{\frac{1}{3}}(\zeta_1 x+\zeta_2 t)-\xi_0))-\frac{2\vartheta_1}{\vartheta_2}}e^{i(\chi_1 x+\chi_2 t)+\sigma w(t)-\sigma^2 t}. \tag{4.11}$$

Case 3. $\Delta = \eta_1^2 - 4\eta_0 > 0$, $\eta_0 \neq 0$.

Assuming $\delta_1 < \delta_2 < \delta_3$, where one is zero and the other two are roots of polynomial $F(\Xi) = \Xi^2 + \eta_1\Xi + \eta_0$, then when $\delta_1 < \Xi < \delta_2$, we can obtain

$$\mathrm{u}_8(x,t) = \pm\sqrt{(-2\vartheta_2)^{-\frac{1}{3}}[\delta_1+(\delta_2-\delta_1)\mathbf{sn}^2(\frac{\sqrt{\delta_3-\delta_1}}{2}((-2\vartheta_2)^{\frac{1}{3}}(\zeta_1 x+\zeta_2 t)-\xi_0),m)]}e^{i(\chi_1 x+\chi_2 t)+\sigma w(t)-\sigma^2 t}, \tag{4.12}$$

where $m = \frac{\delta_2-\delta_1}{\delta_3-\delta_1}$.

When $\Xi > \delta_3$, we can obtain

$$\mathrm{u}_9(x,t) = \pm\sqrt{(-2\vartheta_2)^{-\frac{1}{3}}\frac{-\delta_2\mathbf{sn}^2(\frac{\sqrt{\delta_3-\delta_1}}{2}((-2\vartheta_2)^{\frac{1}{3}}(\zeta_1 x+\zeta_2 t)-\xi_0),m)+\delta_3}{\mathbf{cn}^2(\frac{\sqrt{\delta_3-\delta_1}}{2}((-2\vartheta_2)^{\frac{1}{3}}(\zeta_1 x+\zeta_2 t)-\xi_0),m)}}e^{i(\chi_1 x+\chi_2 t)+\sigma w(t)-\sigma^2 t}. \tag{4.13}$$

Case 4. $\Delta = \eta_1^2 - 4\eta_0 < 0$, $\Xi > 0$.

When $\Xi > 0$, we can obtain the solution of Eq (1.1)

$$\begin{aligned}\mathrm{u}_{10}(x,t) &= \pm\sqrt{(-2\vartheta_2)^{-\frac{1}{3}}\frac{4\sqrt{2\vartheta_0(-2\vartheta_2)^{-\frac{1}{3}}}}{1+\mathbf{cn}^2(8\vartheta_0(-2\vartheta_2)^{-\frac{1}{3}})^{\frac{1}{4}}((-2\vartheta_2)^{\frac{1}{3}}(\zeta_1 x+\zeta_2 t)-\xi_0),n)}-2(-2\vartheta_2)^{-\frac{1}{3}}\sqrt{2\vartheta_0(-2\vartheta_2)^{-\frac{1}{3}}}}\\ &\quad e^{i(\chi_1 x+\chi_2 t)+\sigma w(t)-\sigma^2 t},\end{aligned} \tag{4.14}$$

where $n^2 = \frac{1-\frac{\eta_1}{2\sqrt{\eta_0}}}{2}$.

5. Numerical simulation

In this section, we plot the modulus of the solution $\mathrm{u}_1(x,t)$ based on different parameters when $\zeta_1 = -1, \zeta_2 = -\frac{3}{2}, \gamma_1 = 1, \gamma_2 = \gamma_3 = -\frac{3}{4}, \chi_1 = 1, \chi_2 = -1$, and $\xi_0 = 0$ as shown in Figure 12. In fact, in Figure 12(d), the mode length of $\mathrm{u}_1(x,t)$ is a hyperbolic function solution, which in physics represents a twisted solitary wave solution. However, in Figure 12 (a)–(c), due to the influence of random factors, the solution of $\mathrm{u}_1(x,t)$ appears to be random. Moreover, we plot the modulus of the solution $\mathrm{u}_3(x,t)$ of Eq (1.1) for $\zeta_1 = 1, \zeta_2 = -\frac{1}{2}, \gamma_1 = 1, \gamma_2 = \frac{7}{4}, \gamma_3 = -\frac{1}{4}, \chi_1 = -1, \chi_2 = -1, \vartheta_0 = \frac{1}{8}$ and $\xi_0 = 0$ as shown in Figure 13. In fact, in Figure 13(d), the mode length of $\mathrm{u}_3(x,t)$ is a periodic function solution, which is represented as a periodic solution in physics. However, in Figure 13(a)–(c), due to the influence of random factors, the solution of $\mathrm{u}_3(x,t)$ appears to be random. When the noise intensity $\sigma = 0$, the system degenerates into a deterministic nonlinear Kodama equation, whose solution exhibits a smooth and regular traveling wave structure, such as typical soliton solutions or periodic wave solutions. For example, in Figures 12(d) and 13(d), the solutions that are not affected by noise exhibit clear hyperbolic function structures (representing solitons) and periodic oscillation structures (representing periodic waves), respectively, reflecting the predictability and stability of deterministic systems. However, when $\sigma > 0$, the introduction of noise significantly alters the behavior of the solution. As shown in Figures 12(a)–(c) and 13(a)–(c), the waveform of the solution changes as σ increases.

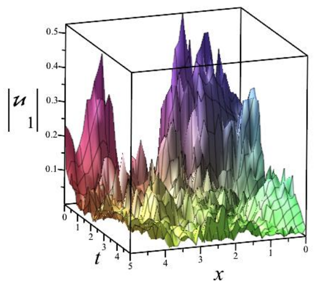

(a) $\sigma = \frac{1}{2}$

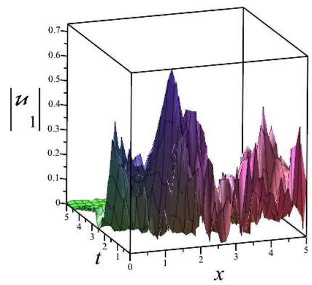

(b) $\sigma = 1$

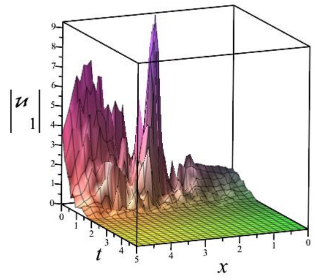

(c) $\sigma = 2$

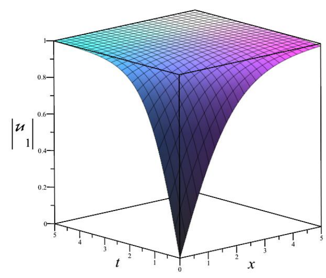

(d) $\sigma = 0$

Figure 12. The modulus of the solution $\mathrm{u}_1(x,t)$ of Eq (1.1) for $\zeta_1 = -1, \zeta_2 = -\frac{3}{2}, \gamma_1 = 1, \gamma_2 = \gamma_3 = -\frac{3}{4}, \chi_1 = 1, \chi_2 = -1, \vartheta_0 = \frac{1}{8}$ and $\xi_0 = 0$.

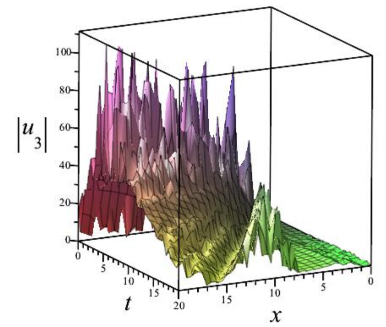

(a) $\sigma = \frac{1}{2}$

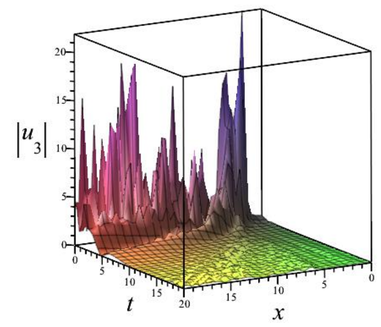

(b) $\sigma = 1$

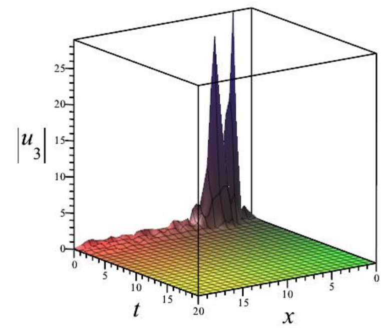

(c) $\sigma = 2$

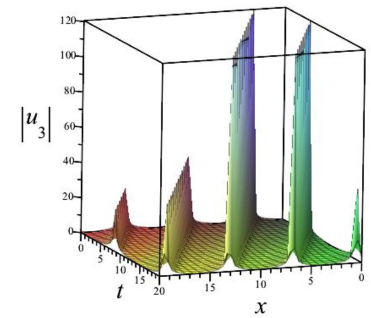

(d) $\sigma = 0$

Figure 13. The modulus of the solution $u_3(x, t)$ of Eq (1.1) for $\zeta_1 = 1, \zeta_2 = -\frac{1}{2}, \gamma_1 = 1, \gamma_2 = \frac{7}{4}, \gamma_3 = -\frac{1}{4}, \chi_1 = -1, \chi_2 = -1, \vartheta_0 = \frac{1}{8}$ and $\xi_0 = 0$.

6. Conclusions

This article uses the planar dynamical system analysis method and the polynomial complete discriminant system method to study the dynamic behavior and traveling wave solutions of SNLK equation, respectively. We studied the two-dimensional dynamical system and its perturbation system of Eq (1.1), and also plotted the two-dimensional and three-dimensional phase diagrams of its different perturbation systems. We obtained the traveling wave solutions of Eq (1.1) using the fully discriminative system method. In order to further illustrate the physical characteristics of these solutions, we plotted three-dimensional graphs of partial solutions considering the absence of noise intensity and given different noise intensities. In summary, this article has significant theoretical implications for the qualitative behavior and traveling wave solutions of SNLK equation.

Author contributions

Jin Wang: Methodology, software, writing–review and editing; Zhao Li: Methodology, validation, funding acquisition, writing–review and editing. All authors have read and approved the final version of the manuscript for publication.

Use of Generative-AI tools declaration

The authors declare they have not used Artificial Intelligence (AI) tools in the creation of this article.

Acknowledgments

This research was funded by Open Research Fund Program of Data Recovery Key Laboratory of Sichuan Province (Grant No.DRN2410).

Conflict of interest

The authors declare no conflict of interest.

References

1. Y. H. Yang, K. J. Wang, Dynamics of the new exact wave solutions to the local fractional Vakhnenko-Parkes equation, *Fractals*, 2025. https://doi.org/10.1142/S0218348X25501026
2. K. J. Wang, An effective computational approach to the local fractional low-pass electrical transmission lines model, *Alex. Eng. J.*, **110** (2025), 629–635. https://doi.org/10.1016/j.aej.2024.07.021
3. N. A. Shah, H. A. Alyousef, S. A. EI-Tantawy, R. Shah, J. D. Chung, Analytical investigation of fractional-order Korteweg–De-Vries-Type equations under Atangana–Baleanu–Caputo operator: Modeling nonlinear waves in a plasma and fluid, *Symmetry*, **14** (2022), 739. https://doi.org/10.3390/sym14040739
4. S. Q. Xu, J. Q. Duan, A Taylor expansion approach for solving partial differential equations with random Neumann boundary conditions, *Appl. Math. Comput.*, **217** (2011), 9532–8542. https://doi.org/10.1016/j.amc.2011.03.137
5. B. Kharkongor, P. M. Kharmawlong, S. S. Pohlong, M. C. Mahato. Net transport and stochastic resonance in an underdamped system due to the application of a traveling-wave force-field, *Physica D*, **457** (2024), 133982.
6. E. Ulutas, Travelling wave and optical soliton solutions of the Wick-type stochastic NLSE with conformable derivatives, *Chaos Soliton. Fract.*, **148** (2021), 111052. https://doi.org/10.1016/j.chaos.2021.111052
7. A. C. Cevikel, Optical solutions for the (3+1)-dimensional YTSF equation, *Opt. Quant. Electron.*, **55** (2023), 510. https://doi.org/10.1007/s11082-023-04787-9

8. S. Zhao, Z. Li. The analysis of traveling wave solutions and dynamical behavior for the stochastic coupled Maccari's system via Brownian motion, *Ain Shams Eng. J.*, **15** (2024), 103037. https://doi.org/10.1016/j.asej.2024.103037
9. A. C. Cevikel, Traveling wave solutions of Fordy–Gibbons equation, *Mod. Phys. Lett. B*, **38** (2025), 2450448. https://doi.org/10.1142/S0217984924504487
10. Z. Li, C. Y. Liu, Chaotic pattern and traveling wave solution of the perturbed stochastic nonlinear Schrödinger equation with generalized anti-cubic law nonlinearity and spatio-temporal dispersion, *Results Phys.*, **56** (2024), 107305. https://doi.org/10.1016/j.rinp.2023.107305
11. M. Raheel, A. Bekir, K. U. Tariq, A. Cevikel, Soliton solutions to the generalized (1+1)-dimensional unstable space time-fractional nonlinear Schrödinger model, *Opt. Quant. Electron.*, **54** (2022), 668.
12. M. S. Algolam, A. I. Ahmed, H. M. Alshammary, F. E. Mansour, W. W. Mohammed, The impact of standard Wiener process on the optical solutions of the stochastic nonlinear Kodama equation using two different methods, *J. Low Freq. Noise V. A.*, **43** (2024), 1939–1952. https://doi.org/10.1177/14613484241275313
13. F. N. K. Sağlam, Analytical approaches to the stochastic nonlinear Kodama equation via the impact of multiplicative noise, *Math. Method. Appl. Sci.*, **48** (2025), 15092–15110. https://doi.org/10.1002/mma.70002
14. W. W. Mohammed, F. M. Al-Askar, New stochastic traveling wave solutions for the Kundu–Mukherjee–Naskar equation with random variable coefficients, *Alex. Eng. J.*, **120** (2025), 154–161. https://doi.org/10.1016/j.aej.2025.02.002
15. A. H. Arnous, M. S. Hashemi, K. S. Nisar, M. Shakeel, J. Ahmad, I. Ahmad,et al., Investigating solitary wave solutions with enhanced algebraic method for new extended Sakovich equations in fluid dynamics, *Results Phys.*, **57** (2024), 107369. https://doi.org/10.1016/j.rinp.2024.107369
16. W. W. Mohammed, F. M. Al-Askar, C. Cesarano, Solitary solutions for the stochastic fokas system found in monomode optical fibers, *Symmetry*, **15** (2023), 1433. https://doi.org/10.3390/sym15071433
17. K. Hosseini, F. Alizadeh, E. Hinçal, D. Baleanu, A. Akgül, A. M. Hassan, Lie symmetries, bifurcation analysis, and Jacobi elliptic function solutions to the nonlinear Kodama equation, *Results Phys.*, **54** (2023), 107129. https://doi.org/10.1016/j.rinp.2023.107129
18. X. H. Du, C. S. Liu, New exact traveling wave solutions for compound KdV-Type equation with nonlinear terms of any order, *Commun. Theor. Phys.*, **46** (2006), 787–792. https://doi.org/10.1088/0253-6102/46/5/004